Journal of The Electrochemical Society

CO_2 Electrolysis to CO and O_2 at High Selectivity, Stability and Efficiency Using Sustainion Membranes

JES Focus Issue on Electrocatalysis — In Honor of Radoslav Adzic

CO_2 Electrolysis to CO and O_2 at High Selectivity, Stability and Efficiency Using Sustainion Membranes

Zengcai Liu, Hongzhou Yang, Robert Kutz, and Richard I. Masel[z]

Dioxide Materials Inc., Boca Raton, Florida 33431, USA

Carbon dioxide (CO_2) electrolysis provides a pathway to close the anthropogenic carbon cycle and store renewable energy, but the stability, selectivity, efficiency and rate of such process needs to be improved. In this paper, we explore the use of Sustainion imidazolium-functionalized membranes and ionomers to improve the performance of that process. Potentiometric runs at a fixed current of 200 mA/cm^2 using Sustainion membranes and ionomers showed that one can maintain 98% selectivity at about 3V applied potential for five months, with a voltage increase of only 3 μV/hour. Other runs showed stable performance at 400 and 600 mA/cm^2. These results pave the way for commercialization of CO_2 electrolysis, providing a viable pathway to recycle CO_2 back to fuels.
 [DOI: 10.1149/2.0501815jes]

Manuscript submitted July 6, 2018; revised manuscript received November 12, 2018. Published November 30, 2018. *This paper is part of the JES Focus Issue on Electrocatalysis — In Honor of Radoslav Adzic.*

Carbon dioxide (CO_2) electrolysis using renewable energy as an input provides a pathway to turn waste CO_2 into valuable fuels and chemicals. It provides a pathway to close the carbon cycle and at the same time to store renewable energy in the form of carbon-containing fuels. There have been many excellent reviews on CO_2 electrolysis,[1–10] but in most previous papers, selectivity values were modest, and currents were low at industrially relevant potentials. Here, selectivity is defined as the ratio of faradaic current derived from formation of desired products (like CO, HCOOH, CH_4...) to total current output during electrolysis.

There are a few cases where industrially relevant currents were seen. For example, Hori et al. achieved a total current density of 100 mA/cm^2 with a CO selectivity of ∼50% on Ag-coated anion exchange membrane electrodes at −2.7 V vs SHE.[11] Verma et al.[12] achieved 440 mA/cm^2 with gas diffusion electrodes at a cell voltage of 3 V by continuously supplying 3 M KOH to the cell without a membrane. Saeki et al. reported a current density of 500 mA/cm^2 with CO selectivity of about 40% on a Cu electrode at a cathode potential of −2.3V (vs Ag quasi-reference electrode) and a pressure of 40 atm in CO_2-methanol medium.[13]

Previously, our group showed[14] that imidazolium salts could lower the onset potential for CO_2 reduction and suppress side reactions, so one can obtain high faradaic efficiencies and low overpotentials. Similar results have been reproduced by other groups.[15–23] However, all of these were done in liquid systems where mass transfer limits performance, so the currents were modest.

To overcome these problems associated with the liquid electrolytes, several researchers attempted to use solid polymer electrolytes instead.[24] Membrane electrode assemblies (MEAs) based on cation exchange membranes (CEM) were first tested for CO_2 reduction, but no or very little current was used to reduce CO_2. Instead, hydrogen was the major product due to the competing reaction of water electrolysis.[25–29] Delacourt et al. achieved a current efficiency of 3% for CO_2 reduction to CO with MEA based on anion exchange membrane (AEM), as compared to 0% with MEA based on CEM.[29] They modified cells with CEM-based MEAs by applying an 800 μm buffer layer of glass fibers impregnated with 0.5M $KHCO_3$ solution between the cathode and CEM. As a result, the faradaic efficiency for CO improved to above 80% at 20 mA/cm^2. Salvatore et al. used a similar cell configuration but replaced the CEM with a bipolar membrane. The faradaic efficiency for CO was about 80% and 50% at 20 mA/cm^2 and 200 mA/cm^2, respectively. They also demonstrated a 24hr run at 100 mA/cm^2 with faradaic efficiency of 65% and a cell voltage of 3.5V.[30] Verma et al.[31] found that both CEM and AEM showed some current for CO_2 reduction on a Cu_2O electrode with a total current efficiency for CO_2 reduction being ∼45% and ∼25% with AEM and CEM, respectively. The current efficiency was further improved up to 80% with KOH doped polyethylenimine/poly(vinyl alcohol) (PEI/PVA/KOH) and quaternized polyethylenimine/poly(vinyl alcohol) (QPEI/PVA/KOH).[32]

Our efforts to incorporate novel solid polymer electrolytes have proved considerably more successful. In continuing our previous work using imidazolium salt in liquid electrolyte, we grafted the imidazolium functional group onto a polymer backbone, resulting in imidazolium-functionalized solid polymer electrolytes: Sustainion anion exchange membranes.[33] A CO_2 electrolyzer with this Sustainion anion exchange membrane showed improved performance, maintaining 50 mA/cm^2 at 3 V with CO selectivity over 90% for over 4000 hours.[33] In this paper, we extended the previous work by optimizing the cathode and achieved 600 mA/cm^2 at 3.3V with over 95% CO selectivity. Most importantly, we have demonstrated that the cell can run at 200 mA/cm^2 below 3V for up to 4000 hours without any significant degradation.[34] As far as we know, we achieved the highest current and selectivity with reasonable electrical energy efficiency and excellent long-term stability.

Experimental

Preparation of sustainion ionomers and membranes.—The Sustainion ionomers were synthesized in a two-step process (Scheme 1): copolymerization of styrene and vinylbenzyl chloride monomers followed by functionalization of resultant copolymer with 1-methyl imidazole.[33] In brief, inhibitor-free styrene (Sigma-Aldrich) (10.058 g, 96.57 mmol) and 4-vinylbenzyl chloride (Sigma-Aldrich) (6.232 g, 40.84 mmol) were mixed in 15 ml of chlorobenzene (Sigma-Aldrich) with 0.1613 g AIBN (α,α′-Azoisobutyronitrile, Sigma- Aldrich) as initiator. The mixture was heated at 60–65°C in an oil bath for 12–18 hours under argon gas.[33] The resultant copolymer -polystyrene vinylbenzyl chloride (PSVBC) was precipitated in CH_3OH/THF (methanol/tetrahydrofuran), washed and dried under vacuum, giving a polymer yield of about 75%. The molecular weight of the PSVBC samples varied from 47,000 to 51,000 atomic units (A.U.) with Polydispersity Index (PDI) between 1.4 and 1.5 as measured with Gel permeation chromatography (GPC). Then, 5.003 g of PSVBC was dissolved in 30 mL of anhydrous N,N-Dimethylformamide (DMF) (Sigma-Aldrich) and functionalized by adding 2.865g (0.035mol) of 1-methylimidazole (Sigma-Aldrich). The resultant mixture was stirred at room temperature for 0.5–1 hour, and then heated at 110–120°C for 50 hours to form a polystyrene vinylbenzyl methylimidazolium chloride (PSMIM) solution. PSMIM was precipitated in ethyl acetate

[z]E-mail: zengcai.liu@dioxidematerials.com; rich.masel@dioxidematerials.com

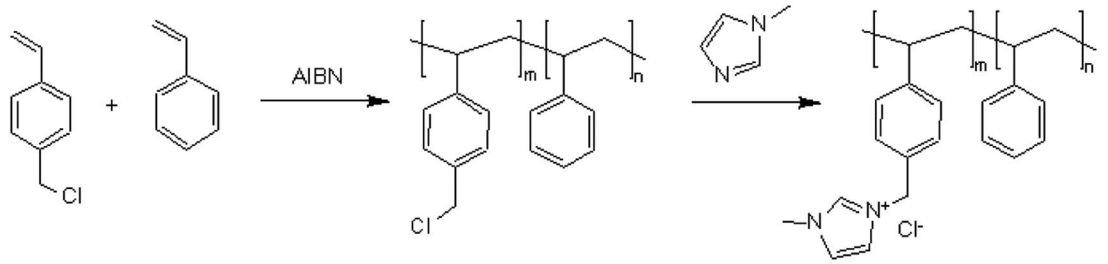

Scheme 1. Synthesis of polystyrene vinylbenzyl chloride (PSVBC) and polystyrene vinylbenzyl methylimidazolium chloride (PSMIM) via copolymerizing styrene and 4-vinyl benzyl chloride followed by functionalizing with 1-methylimidazole.

and washed with ethyl acetate three times to remove any impurities. The resultant PSMIM was dried at 60°C in an oven overnight and re-dissolved in ethanol to make a Sustainion XA7 ionomer solution containing 5% PSMIM. In order to improve the mechanical strength of the membrane, we added divinylbenzene (DVB) as a cross-linking agent during the second step forming a PSMIM-DVB solution. PVBC, PSMIM and PSMIM-DVB were characterized with NMR spectrometer.

Sustainion X24 membranes were prepared by the solution-casting and evaporation method. The polymer solutions containing 15–30% PSMIM-DVB were cast onto glass slides and dried in a vacuum oven at 80°C for 1 hour then 150°C for another hour. The thickness of Sustainion X24 membrane was about 60 μm. The dried membranes were released from the glass slides by soaking the glass slides in 1 M KOH at room temperature. The membranes were allowed to exchange the chloride ions with hydroxide ions by soaking in 1 M KOH for at least 12–24 hours. The membranes were rinsed thoroughly with deionized water before use.

Ionic conductivity measurement.—Through-plane ionic conductivity was measured by using a Potentiostat (Solartron 1287) coupled with Frequency Response Analyzer (FRA 2550). One piece of Sustainion X24 membrane was sandwiched between Pt and IrO_2 electrodes and mounted in a fuel cell hardware coupled with heaters (Fuel Cell Technologies, Albuquerque, NM). Then, 1M KOH was circulated at 1mL/min into both flow fields. The cell temperature was controlled at 25–80°C using a PID controller. The electrochemical impedance spectrum was taken by sweeping AC frequency from 100 k to 100 Hz. The intercept of the complex spectrum at the real axis was used as the resistance (R) to calculate the ionic conductivity (σ) using the following equation:

$$\sigma = \frac{L}{RS} \quad [1]$$

Where L and S are the thickness of the membrane and the geometric area of the electrodes, respectively.

Electrochemical characterization.—Electrodes were prepared by applying nanoparticle inks to porous substrates. The cathode ink was made by dispersing 30 mg of Ag nanoparticles (20nm, US-Nano) and a certain amount of carbon powder (XC-72, Fuel Cell Earth) to a mixture of 0.1 mL distilled water and 0.2 mL isopropanol. The mixture was sonicated for one minute, and then spray-coated onto a 2.5 cm × 2.5 cm square cut of carbon gas diffusion layer (Sigracet 35 BC GDL, Ion Power). For the electrode containing carbon powder and Sustainion XA7 ionomer, Ag nanoparticles and carbon powder were dispersed in ethanol containing the Sustainion XA7 ionomer. Then the cathode ink was spray-coated onto 35BC GDL. Weight percentages of carbon (X wt%) and Sustainion XA7 ionomer (Y wt%) were based on the weight of the Ag nanoparticles, and the electrode was labeled as Ag/X/Y. In these cases, the cathodes were dried in an oven at 80°C for 20 minutes and 120°C for 20 minutes, and then allowed to soak in 1 M KOH for 1 hour in order to exchange Cl^- in the ionomer with OH^-. The actual Ag loading was about 2.0 mg/cm^2. IrO_2 anodes were prepared in the same way as the 'pure' Ag cathode (without carbon and Sustainion XA7 ionomer), but with the addition of 5% Nafion (100 μL) dispersion as binder. The anode catalyst was then dried in an oven for 30 min at 80°C and the IrO_2 loading was about 2 mg/cm^2.

Electrochemical cells were assembled by sandwiching one piece of Sustainion X24 membrane between a Ag cathode and an IrO_2 anode with both catalyst layers facing the membrane. This membrane electrode assembly was then mounted into Fuel Cell Technologies 5 cm^2 fuel cell hardware with serpentine flow channels and gaskets on both sides (Figure 1). CO_2 was humidified at room temperature and supplied to the cathode flow field at 30ccm with a mass flowmeter controller, and deionized water or 10 mM $KHCO_3$ was circulated through the anode flow field via a peristaltic pump. The cell was operated at room temperature (without external heating). Cyclic voltammograms were conducted by scanning the voltage at a rate of 100 mV/s from 1.2 to 3V or until the current reached the maximum current of the Potentiostat. For long term tests, the cell was either set to constant voltage using a Potentiostat, or set at a constant current using a power supply (B&K Precision, Yorba Linda, CA), and the current and voltage were monitored and recorded, respectively. The cathode and anode output gas compositions were analyzed with an Agilent 6890 gas chromatograph with a thermal conductivity detector (GC-TCD) (Agilent Technologies, Santa Clara, CA) equipped with a Carboxen 1010 P LOT GC column (30 m × 320 um) (Sigma Aldrich).

Results and Discussion

Verifying successful synthesis of Sustainion ionomers.—Sustainion XA7 was synthesized by a two-step process. In step one, a random copolymer of styrene and vinyl-benzyl chloride was formed, and was labeled as PSVBC which was characterized by ^{1}H NMR and identified by the proton peak from CH_2Cl at 4.5 ppm (Figure 2A).[35] In step two, PSVBC was functionalized with imidazolium, and polystyrene imidazolium chloride was formed and abbreviated as PSMIM-Cl and labeled as Sustainion XA7. As shown in Figure 2B, a new proton peak appeared at 5.3 ppm indicating successful functionalization with imidazolium. The proton peak from CH_2Cl became smaller and a proton peak at 3.8 ppm

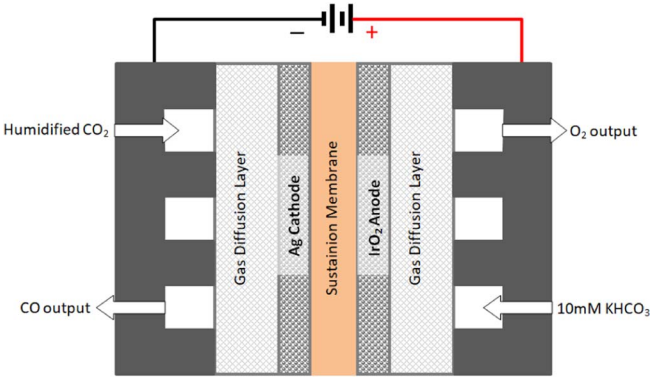

Figure 1. Schematic of CO_2 electrolyzer.

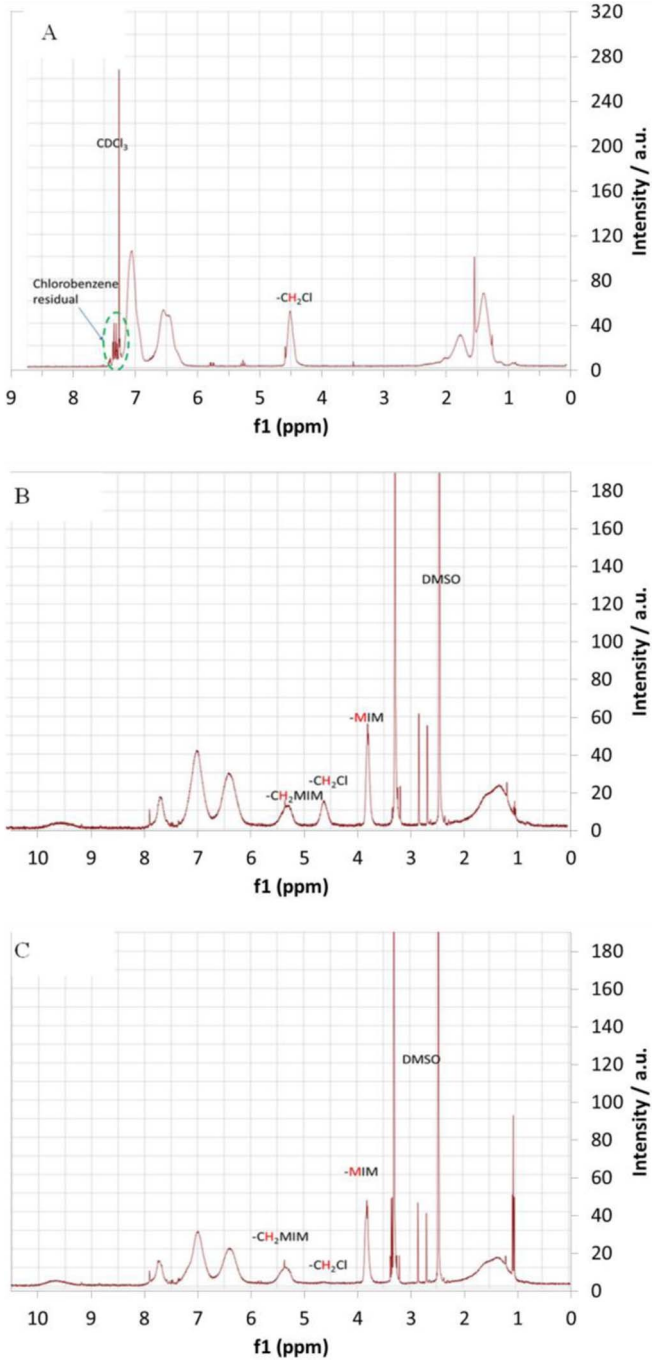

Figure 2. ^{1}H NMR of (A) PSVBC in $CDCl_3$, (B) PSMIM-Cl in DMSO, and (C) PSMIM-Cl/DVB in DMSO.

appeared due to the un-reacted imidazolium. The calculation showed that 51% of -CH_2Cl turned into -CH_2MIM group. In order to improve the mechanical strength of the membrane, we added divinylbenzene (DVB) as cross-linking agent during the second step, forming PSMIM-Cl/DVB and labeled as Sustainion X24. The NMR spectrum (Figure 2C) showed a very weak proton peak from CH_2Cl at 4.6 ppm, and the calculation gave an 88% conversion of -CH_2Cl to -CH_2MIM group.

Ionic conductivity of sustainion membranes.—Figure 3 shows the conductivity of Sustainion X24 membrane as function of the reciprocal of absolute temperature in 1M KOH and 1M $KHCO_3$. The hydroxide ion conductivity was 64 mS cm^{-1} at room temperature and

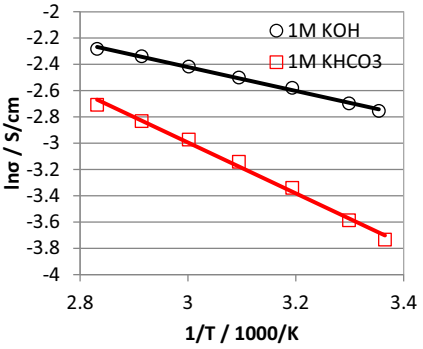

Figure 3. Arrhenius plots of Sustainion X-24 in 1M KOH and 1M $KHCO_3$. Symbols: experiment data. Solid lines: Fitting data.

increased to 102 mS cm^{-1} at 80°C in 1M KOH. The conductivity was 6 times higher than QPEI/PVA/KOH (10 mS cm^{-1}) used for CO_2 electrolyzers,[32] and 1.5 times higher than the best competitive AEM membrane developed by Tokuyama.[36] The activation energy was 7.54 kJ mol^{-1}, which was lower than that reported in literature.[37,38] The high conductivity is most likely related to the random copolymerization process, in which an interconnected hydrophilic region is formed after functionalization with imidazolium. The random copolymer also tends to form an amorphous phase, which better favors ionic conduction when compared to crystalline polymers.[39,40] Our XRD results did not show any crystalline phase (data not shown). In alkaline CO_2 electrolyzers, at least some of the OH^- ions react with CO_2, thus forming HCO_3^- and/or CO_3^{2-}. Therefore, ionic conductivity was also measured in 1M $KHCO_3$. As a comparison, the HCO_3^- conductivity values were 24 and 66 mS cm^{-1} at room temperature and 80°C, respectively. The activation energy for HCO_3^- conduction was 16.1 kJ mol^{-1}. The lower conductivity and higher activation energy in 1M $KHCO_3$ were attributed to the larger resulting ratio of HCO_3^- to OH^-. The conduction mechanism is under investigation.

CO_2 conversion to CO with Sustainion membrane.—The mechanism of alkaline CO_2 reduction and its practical challenges are detailed here (Figure 4). In an alkaline CO_2 electrolyzer, CO_2 is reduced to CO (Eq. 2) at the cathode, with a side reaction of hydrogen production (Eq. 3) from water electrolysis.[24] Both reactions generate OH^- anions that transport through the anion exchange membrane from the cathode to the anode, and O_2 is produced at the anode (Eq. 4). All electrode

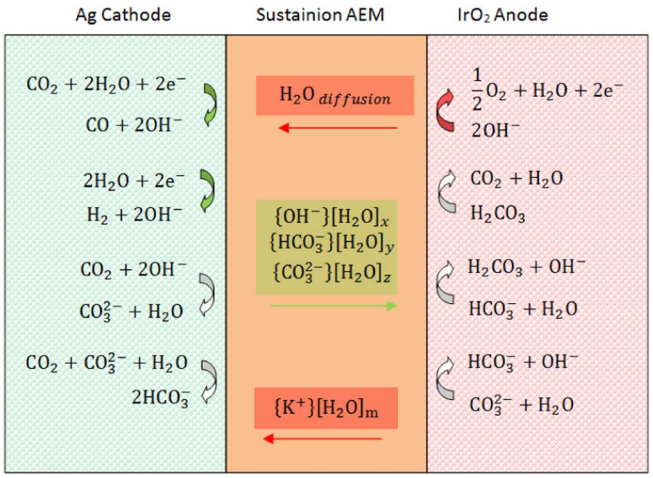

Figure 4. Proposed electrochemical/chemical reactions, ionic species and water transport in CO_2 electrolyzer. Humidified CO_2, and 10 mM $KHCO_3$ are fed to cathode and anode, respectively.

potentials are referred to the reversible hydrogen electrode (RHE).

$$2CO_2 + 2H_2O + 4e^- \rightleftharpoons 2CO + 4OH^- \quad E^0_{c1} = -0.1V \qquad [2]$$

$$4H_2O + 4e^- \rightleftharpoons 2H_2 + 4OH^- \quad E^0_{c2} = 0\ V \qquad [3]$$

$$4OH^- \rightleftharpoons 2H_2O + O_2 + 4e^- \quad E^0_a = 1.23\ V \qquad [4]$$

The overall reactions of CO_2 and water electrolysis are written in Eqs. 5 and 6, respectively.

$$2CO_2 \rightleftharpoons 2CO + O_2 \quad E^0_1 = 1.33\ V \qquad [5]$$

$$2H_2O \rightleftharpoons 2H_2 + O_2 \quad E^0_2 = 1.23\ V \qquad [6]$$

CO selectivity (%) is defined as:

$$Selectivity\ (\%) = \frac{i_{CO}}{i_{CO} + i_{H_2}} \times 100\% \qquad [7]$$

where i_{CO} is the partial current for CO production from CO_2 electrolysis (Eq. 2), and i_{H2} is the partial current for H_2 production from water electrolysis (Eq. 3).

Here, we developed Sustainion anion exchange membranes (AEM) with the dual aims of 1) lowering the overpotential in the same way that EMIM in liquid electrolyte does and 2) simplifying the cell configuration. However, in the presence of CO_2, it is inevitable to form CO_3^{2-} and/or HCO_3^- by neutralizing OH^- in AEM (Eqs. 8 and 9). The neutralization of AEM is very fast, and almost all OH^- ions in AEM change to CO_3^{2-} and/or HCO_3^- within 30min, even when just exposed to air.[41] As a result, pH at the membrane interface decreases, which actually improves the stability of AEM as compared to the high pH in OH^- form.[42]

$$CO_2 + 2OH^- \rightleftharpoons CO_3^{2-} + H_2O \qquad [8]$$

$$CO_2 + CO_3^{2-} + H_2O \rightleftharpoons 2HCO_3^- \qquad [9]$$

Furthermore, both Eqs. 2 and 3 generate OH^- at cathode, leading to the increase in the local pH. Therefore, there are acid-base reactions in the presence of CO_2 (Eqs. 8 and 9) which produce CO_3^{2-} and HCO_3^- in a similar way as the neutralization of OH^- in the membrane with CO_2. Therefore, cathode reaction (Eq. 1) can be rewritten as Eqs. 10 and 11. All anions including OH^-, CO_3^{2-} and HCO_3^- serve as charge carriers in the membrane, and transport from the cathode to the anode.

$$4CO_2 + 4e^- \rightleftharpoons 2CO + CO_3^{2-} \qquad [10]$$

$$6CO_2 + 4e^- \rightleftharpoons 2CO + 4HCO_3^- \qquad [11]$$

Meanwhile, we feed 10 mM $KHCO_3$ to the anode chamber to assist ion conduction in the anode catalyst layer where we used Nafion as a binder (a stable anion exchange ionomer is not available at this moment). Therefore, there is a base hydrolysis equilibrium (Eq. 12) in the anolyte so the pH of the anolyte is higher than 7. Once HCO_3^- and CO_3^{2-} anions arrive in the anode, there is also a base hydrolysis equilibrium (Eq. 13). Both continuous supply of HCO_3^- and CO_3^{2-} from cathode and consumption of OH^- (Eqs. 4) in anode push reactions (Eqs. 12 and 13) shift to right direction. Therefore, CO_2 is released in anode as shown in Eq. 14. The overall anode reactions can be rewritten as Eqs. 15 and 16.

$$HCO_3^- + H_2O \rightleftharpoons OH^- + H_2CO_3 \qquad [12]$$

$$CO_3^{2-} + H_2O \rightleftharpoons OH^- + HCO_3^- \qquad [13]$$

$$H_2CO_3 \rightleftharpoons CO_2 + H_2O \qquad [14]$$

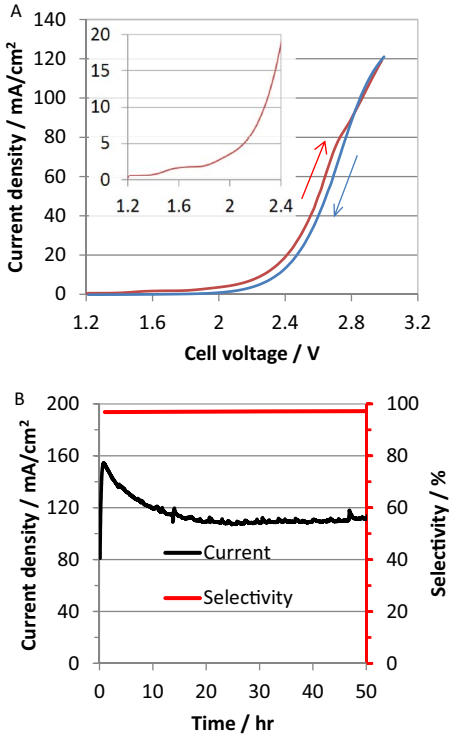

Figure 5. (A) Cyclic voltammogramand (B) Chrono-amperogram and CO selectivity as function of time for a solid CO_2 electrolyzer with only Ag nanoparticle in cathode (Ag/0/0). Inset shows enlarged cyclic voltammogram at lower current.

$$4HCO_3^- \rightleftharpoons 2H_2O + O_2 + 4CO_2 + 4e^- \qquad [15]$$

$$2CO_3^{2-} \rightleftharpoons O_2 + 2CO_2 + 4e^- \qquad [16]$$

Figure 5A shows a typical cyclic voltammogram of the cell with Ag nanoparticles on cathode, IrO_2 on anode, and Sustainion X24 as solid polymer electrolyte. The results show that the current started to increase at ~1.4V and reached a plateau of 2 mA/cm^2 up to 1.8V, then increased rapidly above 1.8V due to the onset of CO_2 reduction (see inset in Figure 5A). The current reached 120 mA/cm^2 at 3V. We did run a cyclicvoltammetry when Ar gas was fed to the cathode rather than CO_2, and the current for hydrogen evolution reached 20 mA/cm^2 at 1.8V. The current was 10 times higher in the absence of CO_2 than in the presence of CO_2. This indicated that the Sustainion membrane also lowers the onset potential for CO_2 reduction and suppress hydrogen evolution in the same way as EMIM solutions.[14,23,43]

Figure 5B shows the chronoamperogram (CA) for the cell at a constant voltage of 3 V. The current reached 150 mA/cm^2 at the beginning and was stabilized at ~100-120 mA/cm^2 after a few hours. We found that CO selectivity was very stable at above 95% for more than 50 hours. Unlike in EMIM-containing ionic liquid, the cell was able to run at a few mA/cm^2 for a few hours.[14] In one of our previous papers, some commercially available membranes were tested in the same setup.[33] All alkaline membrane showed higher selectivity than all acidic membranes, but EMIM containing Sustainion membrane and an imidazole containing H_3PO_4 doped polybenzimidazole (PBI) membrane exhibited the highest CO selectivity among alkaline and acidic membranes, respectively. Apparently, Imidazolium (Imidazole) played a key role in CO_2 reduction. This unique Sustainion membrane improves the current density by more than an order of magnitude and lengthens life time significantly.

By comparison, Delacourt, et al.[29] used polyethersulfone-based AEM with bicylic ammonium groups and reported only 3% faradaic

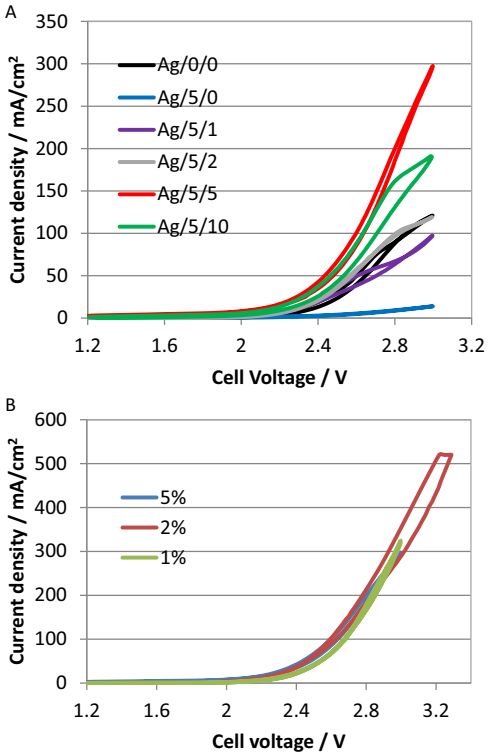

Figure 6. Cyclic voltammograms of solid CO_2 electrolyzer with different Ag cathodes. (A) Ag/x/y refers to an electrode with where the weight percentages of the porous carbon and the Sustainion XA-7 are x and y wt% based on the weight of the silver. (B) Ratio of porous carbon to ionomer was fixed at 1 while the weight of the porous carbon varies between 1–5%.

efficiency on Ag cathode with a total current of 50 mA/cm^2 at a cell voltage of 3V. Hori et al. reported total current of 20–100 mA/cm^2 with Ag coated AEM (Selemion AMV) and 0.2 M K_2SO_4 as anolyte.[11] However, the faradaic efficiency for CO_2 conversion decreased significantly from 95 to 60% when the current increased from 20 to 100 mA/cm^2. In addition, at least two products of CO and HCOOH from CO_2 conversion were identified. The cathode potential was −2.72V (vs SHE) at 100 mA/cm^2, and also shifted negatively to −3.05V (vs SHE) in 2 hour run. Assuming that oxygen was produced on anode, the equilibrium anode potential is 0.81 V at pH of 7. The cell voltage would be 3.53–3.86 V even without contribution of anode overpotential. Figure 5B shows over 100 mA/cm^2 current density with over 95% faradaic efficiency for CO_2 conversion at a cell voltage of 3 V.

Optimization of Ag cathode.—To further improve the rate of CO_2 conversion and its energy efficiency, anion exchange ionomer was introduced into cathode to extend the three phase boundary of Ag catalysts. This technique has precedent in electrodes combined used with a cation exchange ionomer such as Nafion.[44–46] Nafion-bonded Ag cathodes worked in liquid electrolytes for CO_2 electrolysis,[14,34,43] but did not work when the electrode was directly attached to the membrane, as then only hydrogen evolution was dominant. Figure 6A shows the cyclic voltammograms (CVs) of the cells assembled with different cathodes. Porous carbon could be used to improve CO_2 diffusion in the catalyst layer; however, with only porous carbon in Ag cathode (Ag/5/0), the current was even lower than that for Ag/0/0, although the CO selectivity was high. Since only Ag nanoparticles in contact with membrane can be used, most Ag nanoparticles far away from the membrane were wasted. With an increased amount of Sustainion XA-7 in the Ag cathode, the current increased significantly with Ag/5/5 being the most active (red line in Figure 6A). The current density reached 300 mA/cm^2 at 3 V, which was three times higher for Ag/5/5 than for Ag/0/0. The increased current was due to the extended three phase boundary's improvement to Ag utilization.[44] Further increasing Sustainion XA7 in the Ag cathode caused the current to begin decreasing because CO_2 diffusion was limited by too much Sustainion XA7 in cathode.[44] We also ran the cell with only Sustainion XA-7 in the Ag cathode. Unfortunately, the current and the selectivity were low due to the blocking effect of the Sustainion XA-7 polymer since CO_2 diffusion was limited without porous carbon.

Figure 6B shows the cyclic voltammograms for the cell with different amounts of porous carbon while the weight ratio of porous carbon to Sustainion XA-7 was fixed at 1:1. When the amount of porous carbon and Sustainion XA-7 decreased from 5 to 2%, the current was slightly lower at voltages below 2.5 V, but it improved at voltages above 2.5V. The current reached 330mA/cm^2 and 520 mA/cm^2 at 3 and 3.3V, respectively. After further decreasing porous carbon and Sustainion XA-7 amounts to 1%, the current decreased significantly at voltages below 2.8 V, but still rose to 320 mA/cm^2 at 3V. This indicated that CO_2 diffusion was dominant at high current, and CO_2 diffusion was improved by engineering short diffusion paths in which the thickness of catalyst layer was reduced by incorporating less porous carbon and Sustainion XA-7 ionomer.

Life time test.—Figure 7 shows the results of long-term tests with optimized cathode (Ag/2/2) at current densities of 200–600 mA/cm^2. At a current density of 200 mA/cm^2, CO selectivity was about 98% for the entire five-month run, and CO_2 utilization was about 25% at 30 ccm of CO_2. The cell voltage was slowly increasing, but a fit to the data shows that the cell voltage only rose by 3μV/hr over the run. We previously ran a cell at a relatively low current density of 50mA/cm^2 for up to 4000 hours with stable selectivity. A comparison of the earlier results to those in Figure 7A shows that both cell performance and the stability were improved when a mixture of carbon and Sustainion XA-7 was added to the catalyst layer.

We also ran the cell at higher current density (Figure 7B and 7C). At a current density of 400mA/cm^2, the cell voltage increased slightly from 3.1 to 3.2V in 72 hours (3 days) while the selectivity decreased slightly to 95%. This result is likely associated with membrane drying out. At 600 mA/cm^2, the cell voltage varied from 3.2 to 3.3V over a four hour run and the selectivity varied from 93% to 96%.

To the best of our knowledge, this is by far the highest current density with faradaic efficiency of 93% for CO_2 reduction at a cell voltage of 3.2V. Schmidt et al.[47] reported that they needed to apply 6V to the cell to achieve a current of 600 mA/cm^2 with 4M KBr/2.5M KOH as catholyte/anolyte. Verma et al.[12] reported a current density of 160 mA/cm^2 with 3M $KHCO_3$ as sole electrolyte in a membraneless cell. However, no long term tests of Verma's cell were reported so far.

Water management plays key role for lifetime.—It is key to keep membrane hydrated all the time in order for cell to run 4000 hours or longer. We used two strategies to help keeping membrane hydration: 1) humidifying CO_2 and 2) circulating deionized water or diluted $KHCO_3$ solution in the anode. CO_2 was fed at 30ccm through a humidifier at 25°C to the cathode (with active area of 5cm^2), and brought 9.1×10^{-3} g/(cm$^2 \cdot$ h) water into the cathode. However, both CO_2 and water electrolysis (Eqs. 2 and 3) use H_2O as a proton donor. As a result, water consumption would be 6.7×10^{-2} g/(cm$^2 \cdot$ h), which is far more than the water brought in with humidified CO_2. As proposed earlier, all anions including OH^-, HCO_3^- and CO_3^{2-} anions carry water when they transport through anion exchange membranes, much like protons in cation exchange membranes.[48] If OH^-, CO_3^{2-} or HCO_3^- was the only charge carrier in AEM (as shown in Eqs. 4, 15, and 16), the ratio of CO_2/O_2 in gas output from anode would be 0, 2 or 4, respectively. GC analysis of the gas output from anode showed that the ratio of CO_2/O_2 was close to 2, suggesting that CO_3^{2-} be major charge carrier in Sustainion membrane. The number of water molecules carried per mobile ion is defined as the electro-osmotic drag coefficient (ξ).[48] In addition to the consumption of water in cathode reactions for CO_2 and water electrolysis, water loss due to the transportation of solvated anions from cathode to anode would accelerate

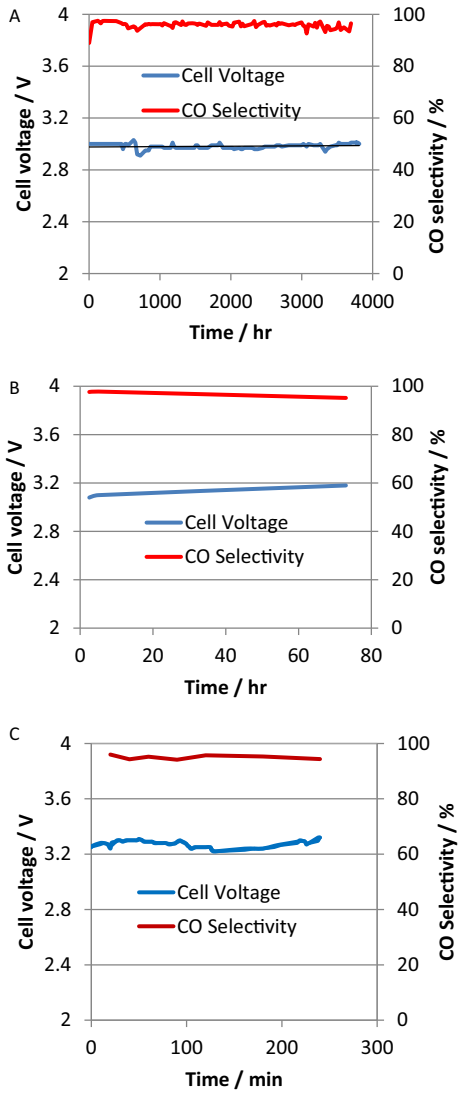

Figure 7. The cell voltage and CO selectivity as function of the time with optimized cathode (Ag/2/2) at (A) 200, (B) 400 and (C) 600 mA/cm^2 and at room temperature.

the dehydration of membrane at the cathode side. Of course, water back diffusion from the anode to cathode helps water management in the membrane. However, if we circulated deionized water in the anode, the cell voltage was stable only for 100 hours or so, and then increased very fast due to the dehydration of the membrane on the cathode side.

Therefore, we circulated 10 mM $KHCO_3$ solution in anode. K^+ ions inevitably transported through the membrane from the anode to the cathode while anions transported from the cathode to the anode. Like anions carry water from cathode to anode, K^+ transportation carry water from anode to cathode that prevent membrane drying-out on cathode side. The exact number of water molecules carried per mobile ion (ξ) in anion exchange membranes is unknown at this stage, and there is very limited data reported for anion exchange membrane in the reference. However, cation (K^+) transported with water molecules from anode to cathode while anions (OH^-, HCO_3^- and CO_3^{2-}) carried water molecules from cathode to anode. This helped water balance in the membrane so that the membrane would not be dehydrated. Therefore, the cell could run up to 4000 hrs with stable cell voltage and CO selectivity. Of course, electroosmotic drag coefficient for all involved anions and cations needs systematic investigation in anion exchange membranes, and expects to play a key role in water management for alkaline membrane CO_2 electrolyzers.

Summary

In summary, a high-conductive anion exchange membrane was developed by functionalization of a copolymer with imidazolium. This anion exchange membrane made CO_2 electrolysis feasible in solid state. Solid CO_2 electrolysis alleviated the flooding problem associated with liquid electrolyte in the cathode, and therefore achieved stable performance. The cell performance was further improved up to 600 mA/cm^2 by successful incorporation of an anion exchange ionomer and a porous carbon into the Ag cathode. The improved performance was attributed to the extended three phase boundaries in Ag cathode. Circulation of diluted $KHCO_3$ in anode play a key role in water management of the membrane, and the cell with optimized cathode can run for up to 3800 hours (158 days) at 200 mA/cm^2 and 3V. We believe that solid CO_2 electrolysis with our anion exchange membrane paves the way for the commercialization of CO_2 conversion to useful chemicals.

Acknowledgments

Parts of this work were supported by ARPA-E under contract DE-AR0000345 and by 3M. The opinions here are those of the authors and may not reflect the opinions of ARPA-E or 3M. Assistance from colleagues, collaborators and friends from 3M are gratefully acknowledged. The authors have received U. S. Patents 9,370,773, 9,481,939, 9,555,367, 9,580,824 which claim the membranes and electrolyzer designs discussed here. Dioxide Materials is planning to offer improved versions of these membranes for sale. The authors all have a financial stake in the outcome of this sale.

ORCID

Zengcai Liu https://orcid.org/0000-0002-0298-6040
Richard I. Masel https://orcid.org/0000-0002-7392-6299

References

1. A. M. Appel, J. E. Bercaw, A. B. Bocarsly, H. Dobbek, D. L. DuBois, M. Dupuis, J. G. Ferry, E. Fujita, R. Hille, and P. J. Kenis, *Chemical reviews*, **113**, 6621 (2013).
2. C. Costentin, M. Robert, and J.-M. Saveant, *Chem. Soc. Rev.*, **42**, 2423 (2013).
3. D. L. DuBois, *Encycl. Electrochem.*, **7a**, 202 (2006).
4. M. Gattrell, N. Gupta, and A. Co, *Journal of Electroanalytical Chemistry*, **594**, 1 (2006).
5. Y. Hori, *Mod. Aspects Electrochem.*, **42**, 89 (2008).
6. J. L. Inglis, B. J. MacLean, M. T. Pryce, and J. G. Vos, *Coord. Chem. Rev.*, **256**, 2571 (2012).
7. E. V. Kondratenko, G. Mul, J. Baltrusaitis, G. O. Larrazabal, and J. Perez-Ramirez, *Energy Environ. Sci.*, **6**, 3112 (2013).
8. R. J. Lim, M. Xie, M. A. Sk, J.-M. Lee, A. Fisher, X. Wang, and K. H. Lim, *Catal. Today*, **233**, 169 (2014).
9. J. Ma, N. Sun, X. Zhang, N. Zhao, F. Xiao, W. Wei, and Y. Sun, *Catalysis Today*, **148**, 221 (2009).
10. J. Qiao, Y. Liu, F. Hong, and J. Zhang, *Chem. Soc. Rev.*, **43**, 631 (2014).
11. Y. Hori, H. Ito, K. Okano, K. Nagasu, and S. Sato, *Electrochimica Acta*, **48**, 2651 (2003).
12. S. Verma, X. Lu, S. Ma, R. I. Masel, and P. J. A. Kenis, *Physical Chemistry Chemical Physics*, **18**, 7075 (2016).
13. T. Saeki, K. Hashimoto, A. Fujishima, N. Kimura, and K. Omata, *The Journal of Physical Chemistry*, **99**, 8440 (1995).
14. B. A. Rosen, A. Salehi-Khojin, M. R. Thorson, W. Zhu, D. T. Whipple, P. J. A. Kenis, and R. I. Masel, *Science*, (2011).
15. J. L. DiMeglio and J. Rosenthal, *J. Am. Chem. Soc.*, **135**, 8798 (2013).
16. Y. Matsubara, D. C. Grills, and Y. Kuwahara, *ACS Catal.*, **5**, 6440 (2015).
17. J. Medina-Ramos, R. C. Pupillo, T. P. Keane, J. L. DiMeglio, and J. Rosenthal, *J. Am. Chem. Soc.*, **137**, 5021 (2015).
18. Y. Oh and X. Hu, *Chem. Commun. (Cambridge, U. K.)*, **51**, 13698 (2015).
19. A. Salehi-Khojin, H.-R. M. Jhong, B. A. Rosen, W. Zhu, S. Ma, P. J. A. Kenis, and R. I. Masel, *J. Phys. Chem. C*, **117**, 1627 (2013).
20. L. Sun, G. K. Ramesha, P. V. Kamat, and J. F. Brennecke, *Langmuir*, **30**, 6302 (2014).
21. F. Zhou, S. Liu, B. Yang, P. Wang, A. S. Alshammari, and Y. Deng, *Electrochem. Commun.*, **46**, 103 (2014).

22. G. P. Lau, M. Schreier, D. Vasilyev, R. Scopelliti, M. Grätzel, and P. J. Dyson, *Journal of the American Chemical Society*, **138**, 7820 (2016).
23. B. A. Rosen, J. L. Haan, P. Mukherjee, B. R. Braunschweig, W. Zhu, A. Salehi-Khojin, D. D. Dlott, and R. I. Masel, *The Journal of Physical Chemistry C*, **116**, 15307 (2012).
24. R. Masel, Z. Liu, D. Zhao, Q. Chen, D. Lutz, and L. Nereng, in *Commercializing Biobased Products: Opportunities, Challenges, Benefits, and Risks*, p. 215, The Royal Society of Chemistry (2016).
25. S. M. A. Kriescher, K. Kugler, S. S. Hosseiny, Y. Gendel, and M. Wessling, *Electrochemistry Communications*, **50**, 64 (2015).
26. R. L. Cook, R. C. MacDuff, and A. F. Sammells, *Journal of The Electrochemical Society*, **135**, 1470 (1988).
27. R. L. Cook, R. C. MacDuff, and A. F. Sammells, *Journal of The Electrochemical Society*, **137**, 187 (1990).
28. D. W. Dewulf and A. J. Bard, *Catalysis Letters*, **1**, 73 (1988).
29. C. Delacourt, P. L. Ridgway, J. B. Kerr, and J. Newman, *Journal of The Electrochemical Society*, **155**, B42 (2008).
30. D. A. Salvatore, D. M. Weekes, J. He, K. E. Dettelbach, Y. C. Li, T. E. Mallouk, and C. P. Berlinguette, *ACS Energy Letters*, **3**, 149 (2018).
31. L. M. Aeshala, R. G. Uppaluri, and A. Verma, *Journal of CO2 Utilization*, **3–4**, 49 (2013).
32. L. M. Aeshala, R. Uppaluri, and A. Verma, *Physical Chemistry Chemical Physics*, **16**, 17588 (2014).
33. R. B. Kutz, Q. Chen, H. Yang, S. D. Sajjad, Z. Liu, and I. R. Masel, *Energy Technology*, **5**, 929 (2017).
34. Z. Liu, R. I. Masel, Q. Chen, R. Kutz, H. Yang, K. Lewinski, M. Kaplun, S. Luopa, and D. R. Lutz, *Journal of CO2 Utilization* (2016).
35. X. Liao, Y. Gong, Y. Liu, D. Zuo, and H. Zhang, *RSC Advances*, **5**, 99347 (2015).
36. Q. Duan, S. Ge, and C.-Y. Wang, *Journal of Power Sources*, **243**, 773 (2013).
37. S. Jeong, J. Lee, S. Woo, J. Seo, and B. Min, *Energies*, **8**, 7084 (2015).
38. T. P. Pandey, H. N. Sarode, Y. Yang, Y. Yang, K. Vezzu, V. D. Noto, S. Seifert, D. M. Knauss, M. W. Liberatore, and A. M. Herring, *Journal of The Electrochemical Society*, **163**, H513 (2016).
39. W. A. Henderson and S. Passerini, *Electrochemistry Communications*, **5**, 575 (2003).
40. A. M. Christie, S. J. Lilley, E. Staunton, Y. G. Andreev, and P. G. Bruce, *Nature*, **433**, 50 (2005).
41. H. Yanagi and K. Fukuta, *ECS Transactions*, **16**, 257 (2008).
42. O. I. Deavin, S. Murphy, A. L. Ong, S. D. Poynton, R. Zeng, H. Herman, and J. R. Varcoe, *Energy & Environmental Science*, **5**, 8584 (2012).
43. B. A. Rosen, W. Zhu, G. Kaul, A. Salehi-Khojin, and R. I. Masel, *Journal of The Electrochemical Society*, **160**, H138 (2013).
44. S. J. Lee, S. Mukerjee, J. McBreen, Y. W. Rho, Y. T. Kho, and T. H. Lee, *Electrochimica Acta*, **43**, 3693 (1998).
45. S. P. Jiang, Z. Liu, and Z. Q. Tian, *Advanced Materials*, **18**, 1068 (2006).
46. S. P. Jiang, Z. Liu, H. L. Tang, and M. Pan, *Electrochimica Acta*, **51**, 5721 (2006).
47. G. Schmid, M. Fleischer, K. Wiesner, and R. Krause, Electrochemical Reduction of CO_2, in (2014).
48. X. Wang, J. P. McClure, and P. S. Fedkiw, *Electrochimica Acta*, **79**, 126 (2012).